Computer-Aided Design (CAD) of Synzymes: Use of Molecular Mechanics (MM) for the Rational Design of Superoxide Dismutase Mimics

Dennis P. Riley,*,† Susan L. Henke, Patrick J. Lennon, and Karl Aston

The Monsanto Company, 800 North Lindbergh Boulevard, St. Louis, Missouri 63167

Received November 16, 1998

Mn(II) complexes of C-substituted macrocyclic 1,4,7,10,13-pentaazacyclopentadecane ligands have been shown to be excellent *functional mimics* (*Synzymes*) of the native enzyme manganese superoxide dismutase (Mn SOD). To better understand the profound effects that substituents exert on the SOD catalytic activity, we have utilized molecular mechanics (MM) calculations employing the CAChe system. Such a conformational analysis has made it possible to develop a consistent model that correlates catalytic rate with the ability of the ligand to adopt a folded geometry about the high-spin d^5 spherically symmetrical Mn(II) ion, thus affording a six-coordinate pseudo-octahedral geometry (the geometry required by Mn(III)). This conformational analysis is consistent with the model that one of the nitrogen donors of the pentaaza crown ligand folds to occupy a pseudo-axial coordination position of an octahedron. The ΔE between the lowest energy folded ligand structure about Mn(II) and its corresponding Mn(III) structure correlates with catalytic activity; i.e., for a large series of complexes an excellent correlation is obtained for both the inner-sphere and outer-sphere rate constants for oxidation of Mn(II)—the rate-determining step in the catalytic cycle for these SOD mimics. From single-crystal X-ray structure determinations on several different members of this class of 7-coordinate dichloro(pentaaza crown) Mn(II) complexes, we have observed that the arrangement of NH's of the secondary amine donors is such that they alternate in their relative orientation to the plane generated by the five nitrogens and the Mn; i.e., the NH's are arranged in an up−down−up−down−up stereochemistry. Thus, one side of the plane of the macrocyclic ring possesses two nonadjacent NH's, while the opposite side has three NH's. Two unique folding motifs generated from MM calculations are found to correlate with the two pathways for Mn(II) oxidation: (1) the inner-sphere path correlates with an NH from the side of the two NH's folding into the axial octahedral coordination site, and (2) the outer-sphere path correlates with an NH from the side of the three NH's folded into an axial O_h site. MM calculations allow one to probe the effect that substituents on the macrocyclic ring carbons have on the relative energies of the Mn(II) and Mn(III) complexes with these ligands in the various potential folded geometries. The details of this modeling paradigm and the results of MM calculations utilizing the folding motif for a large number complexes are described. Of particular significance is the ability of the MM tool to predict correctly that certain substituent patterns and substituents enhance or reduce the contribution of one or the other pathway to the overall catalytic rate. The syntheses of several new complexes are reported and the rate constants for the two pathways of Mn(II) oxidation have been measured and found to correlate with the predictions arising from the energetics of folding as calculated by MM calculations.

Introduction

The pentaaza macrocyclic Mn(II) complex, **1** (Figure 1),[1] and its derivatives bearing substituents on the carbon atoms of the macrocycle[2] are highly active and stable superoxide dismutase (SOD) mimics. Our goal has been the design and synthesis of low molecular weight functional enzyme mimics (*Synzymes*[3,4]) of superoxide dismutase as human pharmaceuticals in an attempt to eliminate some of the drawbacks associated with the use of high molecular weight peptide-based pharmaceuticals, e.g., cost, immunogenicity, tissue penetration, oral bioavailability, etc. In numerous biological studies both in vitro and in vivo, the Mn(II) complexes of this class display potent mechanism-based biological effects.[5] Successful implementation of these metal-based drugs as human pharmaceutical agents mandates that the molecules possess high inherent chemical stability while retaining high SOD activity. Increasing the number of substituents

† Present address: MetaPhore Pharmaceuticals, Inc., 3655 Vista Ave., St. Louis, MO 63110.

(1) Riley, D. P.; Weiss, R. H. *J. Am. Chem. Soc.* **1994**, *116*, 387.
(2) (a) Riley, D. P.; Henke, S. L.; Lennon, P. J.; Weiss, R. H.; Neumann, W. L.; Rivers, W. J., Jr.; Aston, K. W.; Sample, K. R.; Rahman, H.; Ling, C.-S.; Shieh, J.-J.; Busch, D. H.; Szulbinski, W. *Inorg. Chem.* **1996**, *35*, 5213. (b) Riley, D. P.; Henke, S. L.; Lennon, P. J.; Weiss, R. H.; Neumann, W. L. *J. Am. Chem. Soc.* **1997**, *119* (28), 6522.
(3) Riley, D. P.; Weiss, R. H. *CATech* **1997**, *1*, 41.
(4) Royer, G. P. *Biotechnol. Ser.* **1986**, *5*, 297−312.
(5) (a) Weiss, R. H.; Flickinger, A. G.; Rivers, W. J.; Hardy, M. M.; Aston, K. W.; Ryan, U. S.; Riley, D. P. *J. Biol. Chem.* **1993**, *268*, 23049−23054. (b) Weiss, R. H.; Riley, D. P.; Rivers, W. J.; Aston, K. W.; Flickinger, A. G.; Hardy, M. M.; Ryan, U. S. Manganese-Based Superoxide Dismutase Mimics: Design, Discovery and Pharmacologic Efficacies. In *The Oxygen Paradox*; Davies, K. J. A., Ursini, F., Eds.; CLEUP University Press: Padova, Italy, 1995; pp 641−651. (c) Weiss, R. H.; Fretland, D. J.; Baron, D. A.; Ryan, U. S.; Riley, D. P. *J. Biol. Chem.* **1996**, *271*, 26149. (d) Kasten, T. P.; Settle, S. L.; Misko, T. P.; Riley, D. P.; Weiss, R. H.; Currie, M. G.; Nickols, G. A. *Proc. Soc. Exp. Biol. Med.* **1995**, *208*, 170−177. (e) Hardy, M. M.; Flickinger, A. G.; Riley, D. P.; Weiss, R. H.; Ryan, U. S. *J. Biol. Chem.* **1994**, *269*, 18535−18540. (f) Kilgore, K. S.; Friedrichs, G. S.; Johnson, C. R.; Schasteen, C. S.; Weiss; R. H.; Riley, D. P.; Ryan, U. S.; Lucchesi, B. R. *J. Mol. Cell. Cardiol.* **1994**, *26*, 995−1006. (g) Black, S. C.; Schasteen, C. S.; Weiss, R. H.; Riley, D. P.; Driscoll, E. M.; Lucchesi, B. R. *J. Pharmacol. Exp. Therapeut.* **1994**, *270*, 1208−1215. (h) Venturini, C. M.; Sawyer, W. B.; Smith, M. E.; Palomo, M. A.; McMahon, E. G.; Weiss R. H.; Riley, D. P.; Schasteen, C. S. In *The Biology of Nitric Oxide*; Moncada, S., Feelisch, M., Busse, R., Higgs, E. A., Eds.; Portland Press: London; 1994; Vol. 3, pp 65−69.

10.1021/ic981319b CCC: $18.00
Published on Web 03/25/1999

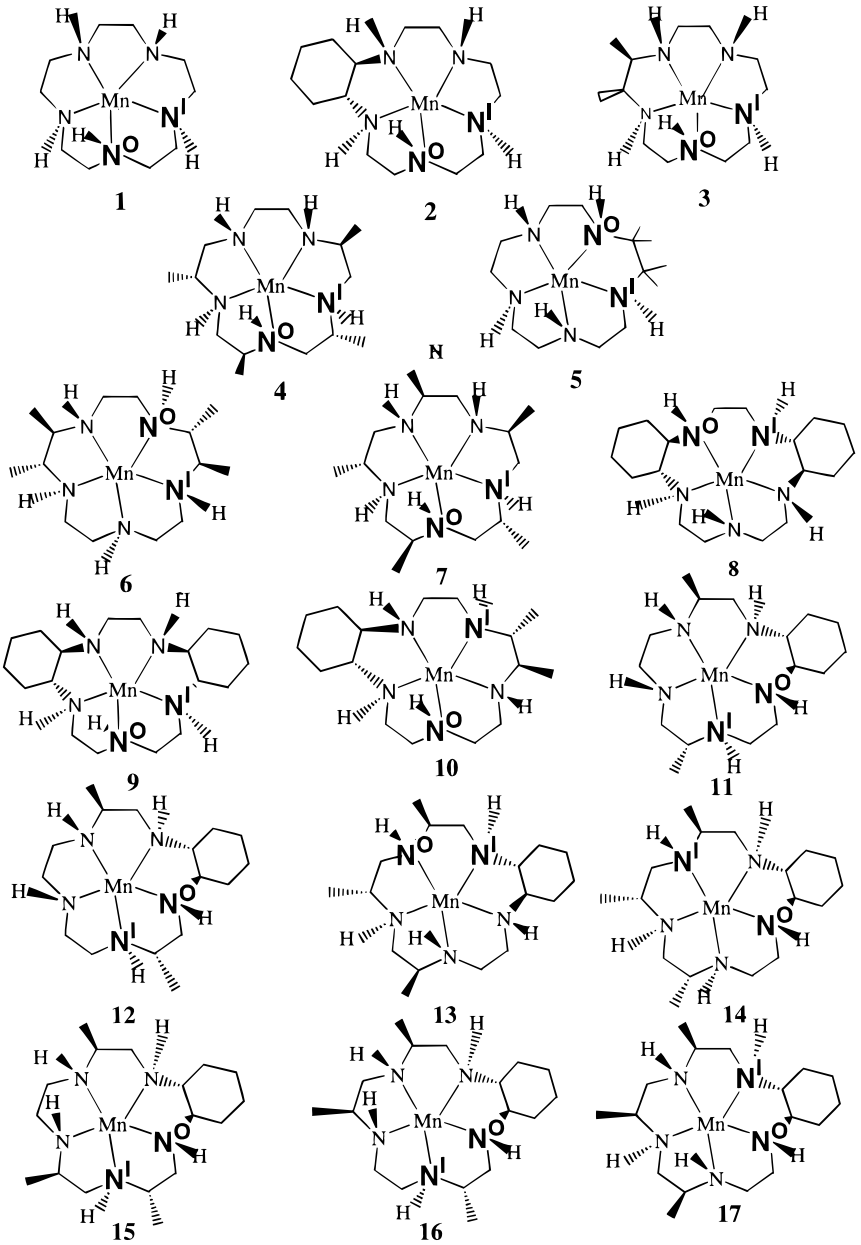

Figure 1. Structures of Mn(II) complexes (axial ligands omitted for clarity) with the macrocyclic ligands utilized for generating a modeling database. The stereochemistry of substituents and NH's is included along with the nitrogen labels: N^O (outer-sphere NH fold) and N^I (inner-sphere NH fold).

on the carbon atoms of the macrocycle invariably increases the stability (both kinetic and thermodynamic) of the Mn(II) complexes derived from **1**,[2] but the number, position, and stereochemistry of the substituents on the carbon atoms of the macrocyclic ring exert a dramatic, and not intuitively apparent, effect on the catalytic SOD activity of the resultant complex. Thus, our goal has been to design an optimum core synzyme structure featuring a maximum number of substituents for maximum chemical stability while retaining the highest achievable catalytic rate. This goal required that we understand the operational details of these catalysts at the molecular level. In an effort to reach a deeper understanding of the mechanism and facilitate the design of optimum structures, we undertook the development of a modeling paradigm that would be consistent and predictive for all structures of this class.

Previously,[2b] we showed that the Mn(II) complexes of these pentaaza crown ligands function via a catalytic cycle in which the rate-determining step is oxidation of Mn(II) to Mn(III). Two independent pathways operate in most of these complexes: (1) an outer-sphere proton-coupled electron transfer from a bound water to an incoming hydroperoxy radical (eq 1):

$$Mn^{II}(L)(OH_2) + HO_2^{\bullet} \xrightarrow[k_1]{} Mn^{III}(L)(OH) + H_2O_2 \quad (1)$$

and (2) an inner-sphere substitution involving coordination of superoxide anion to Mn(II) in a vacant site (eq 2), followed by fast protonation of the bound superoxo creating a pseudo-octahedral Mn(III)−hydroperoxo complex (eq 3):

$$Mn^{II}(L) + O_2^{\bullet -} \xrightarrow[k_2]{} Mn^{II}(L)(OO^-) \qquad \text{(inner-sphere)} \quad (2)$$

$$Mn^{II}(L)(OO^-) + H^+ \xrightarrow[\text{fast}]{} Mn^{III}(L)(O_2H) \quad (3)$$

For either pathway to be maximally efficient requires that the barrier to electron transfer must be minimal; i.e., the ligand

reorganizational barrier to electron transfer must be small.[6,7] Thus, the precursor Mn(II) complex should adopt a six-coordinate pseudo-octahedral geometry similar to that required by the corresponding Mn(III) complex. Thus, loss of an axial ligand followed by folding a secondary amine NH of the macrocyclic ring so that it occupies an axial site would generate a pseudo-octahedral complex, $[Mn^{II}(L)X]^{n+}$, accommodating this requirement of a six-coordinate Mn(II) complex. If the macrocyclic [15]aneN_5 ligand possesses C-substituents, which, due to intramolecular steric repulsions and angle strains, could force the ligand to adopt this folded pseudo-octahedral geometry about the spherically symmetrical Mn(II) ion, then the Mn(II) complex would be poised to undergo facile electron transfer as the ligand reorganizational barrier would be minimized. It is in this manner that the stereochemistry of the substituents would be expected to exert a major effect on the rate of electron transfer via either pathway. This need to rearrange the ligand from a planar geometry into a folded conformation, stabilizing a pseudo-octahedral geometry on Mn(II), may be the reason some complexes of this family, for example, show no measurable rate for one or the other of the two pathways. It is intriguing to speculate that the steric constraints imposed on the folding by the presence of a substituent positioned on a carbon of the ring may favor or inhibit a particular fold and thereby promote or block a particular pathway for electron transfer. This implies that the two mechanisms may operate by different folding motifs.

To better understand the effects that substituents exert, we have utilized a combination of molecular mechanics calculations and synthesis with the goal of rational design of highly substituted chemically stable synthetic enzymes. It needs to be stressed that while the prediction of properties and reactivity of small carbocyclic ring systems based on conformational control is widely practiced and relatively straightforward, the conformational analysis of large macrocyclic ring metal complexes undergoing redox chemistry offers a more difficult challenge.

Experimental Section

Molecular Mechanics. The molecular mechanics (MM) computations were carried out using the program Mechanics implemented on a Tektronix CAChe workstation. This code is based on Allinger's MM-2 molecular mechanics code with extensions provided by the CAChe group.[8] For the Mn(II) complex calculations the structural parameters obtained experimentally from six-coordinate crystal structures were utilized to modify the standard CAChe parameters.[2b] For the Mn(II) complexes the value utilized for R_{av} for the Mn−N distance is 2.283 Å and that for the average Mn−Cl distance, based on that observed from several previous structures,[1,2,9] is 2.616 Å. For the Mn(III) complexes the parmeters used were those supplied by CAChe. For the Mn(II) complexes the MM calculations were performed by assuming that there was no hybridization about the metal, i.e., unconfigured. In contrast, the Mn(III) complexes with a d^4 metal ion were assumed to be d^2sp^3 hybridized and hence configured for octahedral geometry. For the purposes of calculating the energy associated with various folded six-coordinate geometries, chloro was utilized as the sixth ligand. The consistent use of the chloro ligand is based on the crystallographic database, and its use is valid over a series of complexes as its contribution to the sum of the energies will be constant throughout a similar series of complexes and hence its contributions to the correlations can be ignored.

Syntheses of Ligands. The ligands of the complexes **1**−**7** were prepared according to the method of ref 2a, those corresponding to complexes **8** and **9** were prepared via the methods of ref 2b, the ligands, corresponding to complexes **10**, **12**, **15**, **16**, and **21**, were prepared according to the methods of ref 10,[11] the ligands, corresponding to complexes **11**, **13** and **14**, and **17**, were prepared according to ref 9,[12] and the ligands corresponding to complexes **18** and **19** were prepared according to the methods of ref 13.[12] The ligand corresponding to complex **20**, 2*R*,3*R*,8*R*,9*R*-bis(cyclohexano)-12,12-dimethyl-1,4,7,10,-13-pentaazacyclopentadecane, was prepared by the method of refs 12 and 13, but glycine ethyl ester was replaced with the methyl ester of α-aminoisobutyric acid in the final macrocyclization step. Thus, the linear tetraamide (structure **9** of ref 13) was reacted with α-aminoisobutyric acid to yield the linear penta nitrogen macrocycle precursor, which was isolated in 92% yield on the 20 g scale (corresponds to structure **10** of ref 13) and then cyclized to the pentaamide (structure **11** of ref 13) with DPPA and subsequently reduced with $LiAlH_4$ to afford the desired pentaaza macrocylic ligand in about 40% yield for the cyclization step.

Synthesis of Complexes. The Mn^{II}(L)dichloro complexes of the ligands reported here were all synthesized by procedures identical to those of ref 2. In each case stoichiometric amounts of ligand were added to methanolic solutions of anhydrous $MnCl_2$.

Dichloro(1,4,7,10,13-pentaazacyclopentadecane)manganese(II), 1, was prepared according to the procedure of ref 1.

Dichloro(2,3-*trans*-cyclohexano-1,4,7,10,13-pentaazacyclopentadecane)manganese(II), 2, was prepared according to the procedure of ref 2a.

Dichloro(2,3-*trans*,*rac*-dimethyl-1,4,7,10,13-pentaazacyclopentadecane)manganese(II), 3, was prepared according to the procedure of ref 2a.

Dichloro(2*S*,5*R*,8*S*,11*R*-tetramethyl-1,4,7,10,13-pentaazacyclopentadecane)manganese(II), 4, was prepared according to the procedure of ref 2a.

Dichloro(2,2,3,3-tetramethyl-1,4,7,10,13-pentaazacyclopentadecane)manganese(II), 5, was prepared according to the procedure of ref 2a.

Dichloro(2*R*,3*R*,8*R*,9*R*-tetramethyl-1,4,7,10,13-pentaazacyclopentadecane)manganese(II), 6, was prepared according to the procedure of ref 2a.

Dichloro(2*S*,5*R*,8*S*,11*R*,14*S*-pentamethyl-1,4,7,10,13-pentaazacyclopentadecane)manganese(II), 7, was prepared according to the procedure of ref 2a.

Dichloro(2*R*,3*R*,8*R*,9*R*-bis(cyclohexano)-1,4,7,10,13-pentaazacyclopentadecane)manganese(II), 8, was prepared according to the procedure of ref 2b.

Dichloro(2*R*,3*R*,8*S*,9*S*-bis(cyclohexano)-1,4,7,10,13-pentaazacyclopentadecane)manganese(II), 9, was prepared according to the procedure of ref 2b.

Dichloro(2*R*,3*R*-cyclohexano-8*R*,9*R*-dimethyl-1,4,7,10,13-pentaazacyclopentadecane)manganese(II), 10. The free ligand, 2*R*,3*R*-cyclohexano-8*R*,9*R*-dimethyl-1,4,7,10,13-pentaazacyclopentadecane (408 mg, 1.37 mmol), was added to a hot methanolic solution containing 173 mg of anhydrous $MnCl_2$. The resulting solution was stirred at reflux for 1 min and then stirred for 16 h at room temperature. The solvent was then removed via a vacuum, the resultant white solid was dissolved in 25 mL of hot THF, and the solution was filtered through Celite. The volume of the THF solution was reduced to 2 mL and hot diethyl

(6) Marcus, R. A. *Annu. Rev. Phys. Chem.* **1964**, *15*, 155.
(7) (a) Macartney, D. H.; Thompson, D. W. *Inorg. Chem.* **1989**, *28*, 2199. (b) Endicott, J. F.; Kumar, K.; Ramasami, T.; Rotszinger, F. P. In *Progress in Inorganic Chemistry*; Lippard, S. J., Ed.; Wiley: New York, 1983; Vol. 30, p 141. (c) Creaser, I. I.; Harrowfield, J. M.; Herlt, J.; Sargeson, A. M.; Springborg, J.; Geue, R. J.; Snow, M. R. *J. Am. Chem. Soc.* **1977**, *99*, 3181.
(8) Burkert, U.; Allinger, N. L. *Molecular Mechanics*; ACS Monograph 177; American Chemical Society: Washington, D.C, 1982.
(9) Neumann, W. L.; Franklin, G. W.; Sample, K. R.; Aston, K. W.; Weiss, R. H.; Riley, D. P. *Tetrahedron Lett.* **1997**, *38*, 779.
(10) (a) Lennon, P. J.; Henke, S. L.; Aston, K. W. U.S. Patent 5,721,361. (b) Lennon, P. J.; Rahman, H.; Aston, K. W.; Henke, S. L.; Riley, D. P. *Tetrahedron Lett.* **1994**, *35*, 853.
(11) Lennon, P. J.; Henke, S. L. Full paper to be published.
(12) Neumann, W. L. Full paper to be published.
(13) Neumann, W. L.; Franklin, G. W.; Sample, K. R.; Aston, K. W.; Weiss, R. H.; Riley, D. P.; Rath, Nigam. *Tetrahedron Lett.* **1997**, *38*, 3143.

ether added to the cloud point (25 mL). A white crystalline solid formed and was collected by filtration after 24 h. The solid was washed with diethyl ether and dried in vacuo overnight. The yield was 474 mg (82%). MS (FAB, NBA marix): *m*/*z* 387 $(M - Cl)^+$. Anal. Calcd for $C_{16}H_{35}Cl_2MnN_5$: C, 45.40; H, 8.33; Cl, 16.75; N, 16.54. Found: C, 45.46; H, 8.57; Cl, 15.80; N, 15.95

Dichloro(2*R*,11*R*-dimethyl-5*R*,6*R*-cyclohexano-1,4,7,10,13-pentaazacyclopentadecane)manganese(II), 11. The free ligand, 2*S*,9*R*-dimethyl-5*R*,6*R*-cyclohexano-1,4,7,10,13-pentaazacyclopentadecane (150 mg, 0.505 mmol), was added to a hot methanolic solution containing 63 mg of anhydrous $MnCl_2$. The resulting solution was stirred at reflux for 1 min and then stirred for 16 h at room temperature. The solvent was then removed via a vacuum, the resultant white solid was dissolved in 25 mL of hot THF, and the solution was filtered through Celite. The volume of the THF solution was reduced to 1 mL and hot diethyl ether added (∼5 mL). A white crystalline solid formed and was collected by filtration after 24 h. The solid was washed with diethyl ether and dried in vacuo overnight. The yield was 171 mg (80%). MS (FAB, NBA marix): *m*/*z* 387 $(M - Cl)^+$. Anal. Calcd for $C_{16}H_{35}Cl_2MnN_5$: C, 45.40; H, 8.33; Cl, 16.75; N, 16.54. Found: C, 45.32; H, 8.06; Cl, 16.63; N, 16.05.

Dichloro(2*S*,9*R*-dimethyl-5*R*,6*R*-cyclohexano-1,4,7,10,13-pentaazacyclopentadecane)manganese(II), 12. The free ligand, 2*S*,9*R*-dimethyl-5*R*,6*R*-cyclohexano-1,4,7,10,13-pentaazacyclopentadecane (1.102 g, 3.704 mmol), was added to a hot methanolic solution containing 0.471 g of anhydrous $MnCl_2$. The resulting solution was stirred at reflux for 1 min and then stirred for 16 h at room temperature. The solvent was then removed via a vacuum, the resultant white solid was dissolved in 25 mL of hot THF, and the solution was filtered through Celite. The volume of the THF solution was reduced to 5 mL and hot diethyl ether added to the cloud point (25 mL). A white crystalline solid formed and was collected by filtration after 24 h. The solid was washed with diethyl ether and dried in vacuo overnight. The yield was 1.35 g (86%). MS (FAB, NBA marix): *m*/*z* 387 $(M - Cl)^+$. Anal. Calcd for $C_{16}H_{35}Cl_2MnN_5$: C, 45.40; H, 8.33; Cl, 16.75; N, 16.54. Found: C, 45.58; H, 8.26; Cl, 16.43; N, 16.15.

Dichloro(2*R*,3*R*-cyclohexano-6*S*,9*R*,12*S*-trimethyl-1,4,7,10,13-pentaazacyclopentadecane)manganese(II), 13, was prepared according to the procedure of ref 8.

Dichloro(2*R*,3*R*-cyclohexano-6*S*,9*R*,12*R*-trimethyl-1,4,7,10,13-pentaazacyclopentadecane)manganese(II), 14. The free ligand, 2*R*,3*R*-cyclohexano-6*S*,9*R*,12*R*-trimethyl-1,4,7,10,13-pentaazacyclopentadecane (530 mg, 1.701 mmol), was added to a hot methanolic solution containing 214 mg of anhydrous $MnCl_2$. The resulting solution was stirred at reflux for 1 min and then stirred for 16 h at room temperature. The solvent was then removed via a vacuum, the resultant white solid was dissolved in 25 mL of hot THF, and the solution was filtered through Celite. The volume of the THF solution was reduced to 5 mL and hot diethyl ether added to the cloud point (25 mL). A white crystalline solid formed and was collected by filtration after 24 h. The solid was washed with diethyl ether and dried in vacuo overnight. The yield was 610 mg (82%). MS (FAB, NBA marix): *m*/*z* 401.5 $(M - Cl)^+$. Anal. Calcd for $C_{17}H_{37}Cl_2MnN_5$: C, 46.69; H, 8.53; Cl, 16.21; N, 16.01. Found: C, 46.50; H, 8.50; Cl, 15.98; N, 15.81.

Dichloro(2*R*,3*R*-cyclohexano-6*S*,11*R*,14*S*-trimethyl-1,4,7,10,13-pentaazacyclopentadecane)manganese(II), 15. The free ligand, 2*R*,3*R*-cyclohexano-6*S*,9*R*,14*R*-trimethyl-1,4,7,10,13-pentaazacyclopentadecane (352 mg, 1.13 mmol), was added to a hot methanolic solution containing 142 mg of anhydrous $MnCl_2$. The resulting solution was stirred at reflux for 1 min and then stirred for 16 h at room temperature. The solvent was then removed via a vacuum, the resultant white solid was dissolved in 25 mL of hot THF, and the solution was filtered through Celite. The volume of the THF solution was reduced to 10 mL and hot diethyl ether added to the cloud point (15 mL). A white crystalline solid formed and was collected by filtration after 24 h. The solid was washed with diethyl ether and dried in vacuo overnight. The yield was 352 mg (71%). MS (FAB, NBA marix): *m*/*z* 401.1 $(M - Cl)^+$. Anal. Calcd for $C_{17}H_{37}Cl_2MnN_5$: C, 46.69; H, 8.53; Cl, 16.21; N, 16.01. Found: C, 47.02; H, 8.66; Cl, 15.95; N, 16.03.

Dichloro(2*R*,3*R*-cyclohexano-6*S*,9*S*,14*S*-trimethyl-1,4,7,10,13-pentaazacyclopentadecane)manganese(II), 16. The free liagnd, 2*R*,3*R*-cyclohexano-6*S*,9*R*,14*S*-dimethyl-1,4,7,10,13-pentaazacyclopentadecane (202 mg, 648 mmol), was added to a hot methanolic solution containing 81.5 mg of anhydrous $MnCl_2$. The resulting solution was stirred at reflux for 1 min and then stirred for 16 h at room temperature. The solvent was then removed via a vacuum, the resultant white solid was dissolved in 25 mL of hot THF, and the solution was filtered through Celite. The volume of the THF solution was reduced to 5 mL and hot diethyl ether added to the cloud point (25 mL). A white crystalline solid formed and was collected by filtration after 24 h. The solid was washed with diethyl ether and dried in vacuo overnight. The yield was 162 mg (57%). MS (FAB, NBA marix): *m*/*z* 401.3 $(M - Cl)^+$. Anal. Calcd for $C_{16}H_{35}Cl_2MnN_5$: C, 46.69; H, 8.53; Cl, 16.21; N, 16.01. Found: C, 46.79; H, 8.59; Cl, 16.08; N, 15.91.

Dichloro(2*R*,3*R*-cyclohexano-6*S*,9*S*,12*S*-trimethyl-1,4,7,10,13-pentaazacyclopentadecane)manganese(II), 17. The free ligand, 2*R*,3*R*-cyclohexano-6*S*,9*S*,12*S*-trimethyl-1,4,7,10,13-pentaazacyclopentadecane (109 mg, 350 mmol), was added to a hot methanolic solution containing 43 mg of anhydrous $MnCl_2$. The resulting solution was stirred at reflux for 1 min and then stirred for 16 h at room temperature. The solvent was then removed via a vacuum, the resultant white solid was dissolved in 25 mL of hot THF, and the solution was filtered through Celite. The volume of the THF solution was reduced to 1 mL and hot diethyl ether added to the cloud point (25 mL). A white crystalline solid formed and was collected by filtration after 24 h. The solid was washed with diethyl ether and dried in vacuo overnight. The yield was 112 mg (74%). MS (FAB, NBA marix): *m*/*z* 401.1 $(M - Cl)^+$. Anal. Calcd for $C_{17}H_{37}Cl_2MnN_5$: C, 46.69; H, 8.53.Found: C, 46.46; H, 8.32.

Dichloro(2*R*,3*R*,8*R*,9*R*-bis(cyclohexano)-12*S*-methyl-1,4,7,10,13-pentaazacyclopentadecane)manganese(II), 18. The free ligand, 2*R*,3*R*,8*R*,9*R*-bis(cyclohexano)-12*S*-methyl-1,4,7,10,13-pentaazacyclopentadecane (255 mg, 755 mmol), was added to a hot methanolic solution containing 119 mg of anhydrous $MnCl_2$. The resulting solution was stirred at reflux for 1 min and then stirred for 16 h at room temperature. The solvent was then removed via a vacuum, the resultant white solid was dissolved in 25 mL of hot THF, and the solution was filtered through Celite. The volume of the THF solution was reduced to 2 mL and hot diethyl ether added to the cloud point (25 mL). A white crystalline solid formed and was collected by filtration after 24 h. The solid was washed with diethyl ether and dried in vacuo overnight. The yield was 310 mg (88%). MS (FAB, NBA marix): *m*/*z* 427.3 $(M - Cl)^+$. Anal. Calcd for $C_{19}H_{39}Cl_2MnN_5$: C, 49.25; H, 8.48; N, 15.11. Found: C, 49.73; H, 8.56; N, 15.28.

Dichloro(2*R*,3*R*,8*R*,9*R*-bis(cyclohexano)-12*R*-methyl-1,4,7,10,13-pentaazacyclopentadecane)manganese(II), 19. The free ligand, 2*R*,3*R*,8*R*,9*R*-bis(cyclohexano)-12*R*-methyl-1,4,7,10,13-pentaazacyclopentadecane (500 mg, 1.481 mmol), was added to a hot methanolic solution containing 234 mg of anhydrous $MnCl_2$. The resulting solution was stirred at reflux for 1 min and then stirred for 16 h at room temperature. The solvent was then removed via a vacuum, the resultant white solid was dissolved in 25 mL of hot THF, and the solution was filtered through Celite. The volume of the THF solution was reduced to 2 mL and hot diethyl ether added to the cloud point (25 mL). A white crystalline solid formed and was collected by filtration after 24 h. The solid was washed with diethyl ether and dried in vacuo overnight. The yield was 575 mg (84%). MS (FAB, NBA marix): *m*/*z* 427.3 $(M - Cl)^+$. Anal. Calcd for $C_{19}H_{39}Cl_2MnN_5$: C, 49.25; H, 8.48;Cl, 15.30; N, 15.11. Found: C, 49.03; H, 8.50; Cl, 15.18; N, 14.96.

Dichloro(2*R*,3*R*,8*R*,9*R*-bis(cyclohexano)-12,12-dimethyl-1,4,7,10,-13-pentaazacyclopentadecane)manganese(II), 20. The free ligand, 2*R*,3*R*,8*R*,9*R*-bis(cyclohexano)-12,12-dimethyl-1,4,7,10,13-pentaazacyclopentadecane (680 mg, 1.93 mmol), was added to a hot methanolic solution containing 243 mg of anhydrous $MnCl_2$. The resulting solution was stirred at reflux for 1 min and then stirred for 16 h at room temperature. The solvent was then removed via a vacuum, the resultant white solid was dissolved in 25 mL of hot THF, and the solution was filtered through Celite. The volume of the THF solution was reduced to 2 mL and hot diethyl ether added to the cloud point (25 mL). A white crystalline solid formed and was collected by filtration after 24 h. The solid was washed with diethyl ether and dried in vacuo overnight. The yield was 420 mg (46%). MS (FAB, NBA marix): *m*/*z* 441.3 (M

$- Cl)^+$. Anal. Calcd for $C_{20}H_{41}Cl_2MnN_5$: C, 50.32; H, 8.66; N, 14.67. Found: C, 49.93; H, 8.46; N, 14.48.

Dichloro(2*R*,3*R*,8*R*,9*R*-bis(cyclohexano)-12*R*,15*R*-dimethyl-1,4,7,-10,13-pentaazacyclopentadecane)manganese(II), 21. The free ligand, 2*R*,3*R*,8*R*,9*R*-bis(cyclohexano)-12*R*,15*R*-dimethyl-1,4,7,10,13-pentaazacyclopentadecane (201 mg, 570 mmol), was added to a hot methanolic solution containing 72 mg of anhydrous $MnCl_2$. The resulting solution was stirred at reflux for 1 min and then stirred for 16 h at room temperature. The solvent was then removed via a vacuum, the resultant white solid was dissolved in 25 mL of hot THF, and the solution was filtered through Celite. The volume of the THF solution was reduced to 1 mL and hot diethyl ether added to the cloud point (25 mL). A white crystalline solid formed and was collected by filtration after 24 h. The solid was washed with diethyl ether and dried in vacuo overnight. The yield was 172 mg (63%). MS (FAB, NBA marix): *m*/*z* 441.3 (M $- Cl)^+$. Anal. Calcd for $C_{20}H_{41}Cl_2MnN_5$: C, 50.10; H, 8.66; N, 14.67. Found: C, 50.31; H, 8.61; N, 14.66.

Physical Methods. Kinetic stabilities were determined by the Cu(II) ion competition method described in detail in our previous studies.[2] The method utilized to determine the superoxide dismutase catalytic activity of the Mn(II) complexes reported here is based on the stopped flow kinetic assay described previously.[1,2,3,14] The work described here utilized the same methodology and the k_{cat} for each complex was assessed over the pH range of 7.4−8.3.

Results and Discussion

To effectively develop a rational modeling paradigm not only requires a detailed understanding of the mechanism of the rate-determining step in the catalytic process, but also a comprehensive database of chemical structures with their rate data so that the theoretical model can be subjected to stringent testing. Figure 1 shows the structures of the Mn(II) complexes (the *trans*-dichloro ligands are omitted for clarity) with the stereochemistry of the ligands utilized in this study. Each of these complexes has been completely characterized in terms of physical properties (e.g., the kinetic stability to dissociation in aqueous media) as well as the kinetics of their superoxide dismutase catalytic activity (k_{cat} determined at pH = 7.4).[1,2] In Table 1 are listed the rate constants for SOD activity at pH = 7.4, the measured rate constants for both the inner-sphere pathway (k_{IS}) and the outer-sphere proton-coupled electron transfer (k_{OS}), and k_{diss}, the second-order rate constant for the proton-assisted ligand dissociation (first-order in both [complex] and in $[H^+]$). Clearly, as we noted previously,[2] increasing the number of the substituents on the macrocyclic ligand increases the kinetic stability of the complexes to dissociation in water. To convert the reported k_{diss} value to a half-life at any pH, eq 4 applies.

$$t_{1/2} = 0.694/(k_{diss}[H^+]) \quad (4)$$

Since ischemia reperfusion injury is a disease for which these synzymes are being considered as human pharmaceuticals and since ischemic tissue has been reported to be ∼pH = 5, it is relevant to compare kinetic stabilities at this pH. Thus, the parent unsubstituted complex has a $t_{1/2}$ of 25 s. In contrast, the most highly substituted complex **21** has a $t_{1/2}$ of 49 600 s (or 14 h)—more than adequate kinetic stability to meet the needs of a transient pH lowering. As noted previously, the bis(cyclohexano) complexes **8** and **9** are considerably more stable than **1** (on the order of 100-fold), but stability does not correlate with the catalytic activity since complex **9** has no measurable SOD activity.[2b]

Table 1

complex	k_{diss} (M^{-1} s^{-1})[a]	k_{cat} ($\times 10^7$ M^{-1} s^{-1}, pH = 7.4)[b]	k_{IS} (10^7 s^{-1})[c]	k_{OS} (10^{10} M^{-1} s^{-1})[c]
1	2814	4.13	0.91	0.29
2	1375	9.09	1.44	0.78
3	701	8.84	1.09	0.84
4	83	5.37	1.99	0.17
5	150	2.20	0	0.28
6	131	3.37	1.13	0.14
7	17	3.82	1.91	0
8	28	12.1	1.58	1.12
9	32	0	0	0
10	43	2.96	1.48	0
11		9.10	0.73	1.00
12	97	10.7	1.55	0.97
13	23	3.62	0.98	0.21
14	16	9.56	1.31	0.87
15	38	8.48	1.48	0.36
16	22	7.62	2.10	0.43
17	24	10.8	0.28	1.18
18	4.8	6.13	0.98	0.53
19	4.0	15.0	0.57	1.80
20	5.9	0.3	0.15	0
21	1.4	4.56	0.39	0.45

[a] k_{diss} is the second-order proton-dependent rate constant for the dissociation of the Mn(L) complexes at 21 °C (see ref 2a). [b] Catalytic rate constant for dismutation of superoxide at 21 °C (see refs 1 and 2). [c] The rate law for loss of superoxide is $V = [Mn]^1_{tot}[O_2^{\bullet -}]^1\{k_{H^+}[H^+]^1 + k_{ind}\}$, where $k_{H^+} = 2k_{OS}/K_a$ (K_a is the acidity constant for superoxide) and $k_{ind} = 2k_{IS}$ (see ref 2).

The catalytic activities of the database complexes **1**−**17** follow no apparent trend with the number of substituents or with the stereochemisty, other than that they both clearly have effects on the overall rate and on the two competing pathways for oxidation of Mn(II) during the catalytic cycle. Most striking is that for some of these complexes there is either no measurable inner-sphere or no outer-sphere rate. Complexes **7**, **9**, and **10** have no measurable k_{OS}. It is especially noteworthy since complex **10** has the same number of substituents in the same location and stereochemistry as the highly active outer-sphere catalyst, complex **8**. A striking example of the effect of stereochemistry is also exemplified by complexes **8** and **9**, both of which feature bis(*trans*-cyclohexano) substituents: **8** is highly active, while **9** has no activity! Another interesting contrast is provided by the series of cyclohexano−trimethyl complexes **13**−**17**. Complex **13** has a very low k_{OS} rate, but **14** and **17** have considerably larger values. In contrast, both **13** and **14** have a fast inner-sphere rate, while **17** has a modest k_{IS}.

The complexes **1**−**17** were utilized as the original database to construct the modeling paradigm. Complexes **18**−**21** (Figure 2) were synthesized on the basis of predictions of the model and provided tests of the predictive power of the MM calculations. For the complexes, **18**−**21**, their kinetic stabilities and catalytic rate constants, k_{cat} (pH = 7.4), are also displayed in Table 1.

Modeling. While there are a number of computational methods available that could be used to predict structures and calculate the thermodynamic properties of a given structure for a coordination complex, the simplest level of calculation would be the use of molecular mechanics (MM) assuming appropriate parameters are available.[15] We have completed the structure refinements of many complexes in this class[16] and reported five

(14) Riley, D. P.; Rivers, W. J.; Weiss, R. H. *Anal. Biochem.* **1991**, *196*, 344.

(15) (a) Hancock, R. D. *Acc. Chem. Res.* **1990**, *23*, 253. (b) Wade, P. W.; Hancock, R. D.; Boeyens, J. C. A.; Dobson, S. M. *J. Chem. Soc., Dalton Trans.* **1990**, 483. (c) Luckay, R.; Chantson, T. E.; Riebenspies, J. H.; Hancock, R. D. *J. Chem. Soc., Dalton Trans.* **1995**, 1363.

(16) Unpublished results.

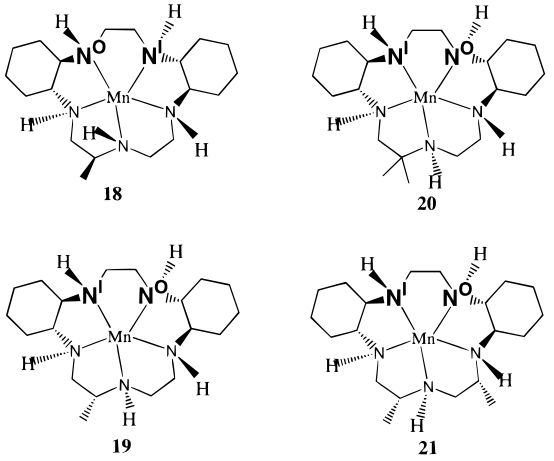

Figure 2. Structures of four Mn(II) complexes (axial ligands omitted for clarity) with the macrocyclic ligands utilized for testing the modeling paradigm. The stereochemistry of substituents and NH's is included along with the nitrogen labels: N^O (outer-sphere NH fold) and N^I (inner-sphere NH fold).

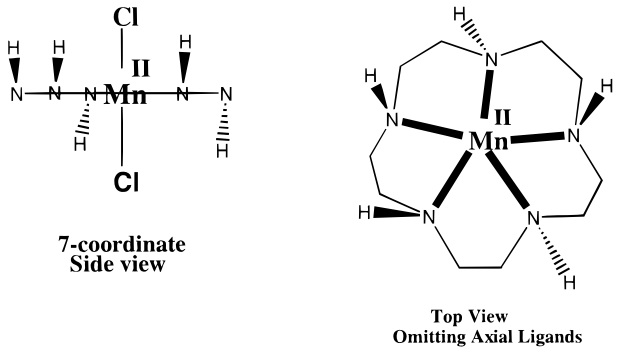

Figure 3. View of Mn(II) pentaaza macrocyclic ligand complex with a stereo depiction of the NH orientation.

crystal structures of this class of Mn(II) pentaaza crown complexes.[1,2,9] This extensive X-ray structural database has allowed us to refine the commercial parameters and utilize an improved R_{avg} for the Mn−nitrogen distance, 2.283 Å, and also an R_{avg} for the Mn−Cl distance, 2.616 Å. Additionally, from these X-ray single crystal structure determinations we have observed in all cases that the NH stereochemical pattern is alternating; i.e., each side of the plane of the macrocyclic ring is chemically unique, since one side will have two nonadjacent NH's, while the other side possesses three NH's (Figure 3) in a cis orientation. This motif provides a basis for probing the structural effects utilizing MM calculations.

The premise that we set out to test developed around the concept that the ligand dictated catalytic activity by promoting or preventing a particular folded structure. Thus, a good catalyst will be one in which the Mn(II) center is constrained in a geometry that promotes rapid electron transfer, i.e., a pseudo-octahedral geometry preferred by Mn(III). Consequently, the folding of an NH out of the plane defined by the metal and the five nitrogens of the ligand into an axial site governs the ability of the corresponding complex to function as a catalyst. The MM calculations can then be utilized to determine the relative energies of all the possible folds for each complex (five possible, since each nitrogen can fold into an axial site, but only on the side of the macrocycle in which the NH is located) and their relative energies compared.

For all the complexes in Table 1 an evaluation of the energy difference (ΔE) of the folded six-coordinate structure of the Mn(II) and corresponding Mn(III) were performed for each NH folded into an axial site. From this evaluation of different folded structures each complex will possess a lowest energy folded structure for the six-coordinate complex derived from an NH on the side of the three NH's occupying a pseudo-axial site, and also a lower energy structure for the six-coordinate complex derived from an NH on the side of two cis nonadjacent NH's occupying a pseudo-axial site. Thus, a correlation of the energy difference, ΔE ($\Sigma_{Mn(III)} - \Sigma_{Mn(II)}$), for a series of complexes for each of the two types of folds (potentially correlating with unique inner-sphere and outer-sphere folded structures) can be performed, where the ground-state energy of both Mn(III) and Mn(II) are approximated by the summation of the various contributing energy terms:[7]

$$\Sigma_{Mn(III)} = U_{electrostatics} + U_{H-bonding} + U_{bond\ stretch} + U_{angle\ strain} + U_{torsional\ strain} + U_{dihedral\ strain} + U_{van\ der\ Waals} + U_{angle\ deformation} \quad (5)$$

and

$$\Sigma_{Mn(II)} = U'_{electrostatics} + U'_{H-bonding} + U'_{bond\ stretch} + U'_{angle\ strain} + U'_{torsional\ strain} + U'_{dihedral\ strain} + U'_{van\ der\ Waals} + U'_{angle\ deformation} \quad (6)$$

For a series of complexes a correlation of ΔE for the folded geometries (inner-sphere and outer-sphere) is simplified by comparing a modified energy $\Delta E^{\#}$ in which the contribution of ($U_{electrostatics} - U'_{electrostatics}$) + ($U_{H-bonding} - U'_{H-bonding}$) are removed since they are maintained invariant among the series of complexes. Plots of $\Delta E^{\#}$ ($\Sigma_{Mn(III)} - \Sigma_{Mn(II)})_{inner-sphere}$ vs k_{IS} values (inner-sphere rate constant), and $\Delta E^{\#}$ ($\Sigma_{Mn(III)} - \Sigma_{Mn(II)})_{outer-sphere}$ vs k_{OS} values (outer-sphere rate constant) can be generated. Linear plots of $\Delta E^{\#}$ vs k_{IS} or k_{OS} would indicate that the correlation is valid. The goal of such a correlation is to determine if (1) the folding paradigm is indeed consistent, and (2) there are unique folding patterns for the inner-sphere and separate unique folding patterns for the outer-sphere pathways, and (3) if the MM calculation/modeling paradigm can be successfully used to predict structures to be synthesized so as to optimize the number of substituents for maximum stability while retaining high catalytic activity.

For any given complex there may exist two mechanistically distinct pathways for oxidation of Mn(II) during the catalytic cycle, though one pathway may predominate. They cannot, however, both be operative simultaneously during a given catalytic cycle. Since profound differences in the measured rate constants are obtained for regio- and stereoisomers, it may be that different intermediate structures are operative for the two separate paths or that the relative energies of analogous Mn(III) structures are quite different. The most likely interpretation is that for each complex a different folding is involved in generating a six-coordinate pseudo O_h Mn(II) complex precursor to electron transfer; i.e., a different NH must fold into the axial site for the inner-sphere and for the outer-sphere path.

Our initial foray into the modeling using MM calculations involved trying to probe the relative energetics of two types of six-coordinate structures generated via loss of a ligand from a *trans*-seven-coordinate Mn(II), as depicted in Figure 4. In solution and solid state both the six- and seven-coordinate geometry exist for these complexes; thus, in solution, a dynamic equilibrium of such structures is expected.[1,2] Two initial six-coordinate structures could be generated via the loss of an axial ligand from the seven-coordinate structure; i.e., the complex labeled **A** in Figure 4, which has the vacant site on the side in

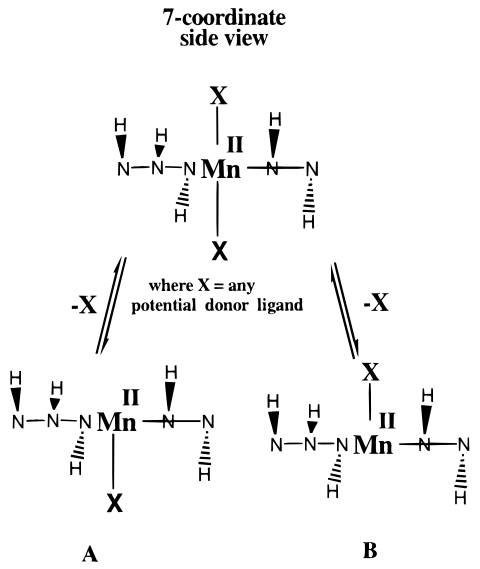

Figure 4. Depiction of the proposed dynamic equilibrium of two possible six-coordinate intermediate structures generated via ligand dissociation from a seven-coordinate *trans* intermediate Mn(II) complex.

which three NH's are cis, and the structure labeled **B**, which has the vacant site on the side with two nonadjacent NH's cis. Clearly, the two intermediates are chemically quite distinct and for each an energy can be calculated using an MM approach. Invariably, the structure **A** with the three NH side containing the vacant site was found to be at a much lower energy than the structure **B** (in the range of 4−8 kcal for chloro as axial ligand and 8−12 for aquo). The magnitude of the difference suggests that structure **A** should be a logical starting point as a common intermediate leading to catalysis for all complexes, i.e., the starting point for productive chemistry during a catalytic cycle. Using this approach and assuming that the six-coordinate aquo complex is the Mn(II) complex in water which leads to productive chemistry,[1,2b] the simplest entry to the outer-sphere pathway presents itself as the aquo complex of structure **A**. This means that for this path to be viable (fast rate) for a given complex, the substituents would force one of the three cis NH's on the side of the vacant coordination site out of the plane defined by the Mn(II) and the five nitrogen atoms (in effect, folded) into the axial pseudo O_h site. When this is investigated for these complexes **1**−**17**, we find, in general, that there is a most preferred NH (lowest energy conformer) folding for one of the three cis NH nitrogens into an axial pseudo O_h site. This is the modeling paradigm that evolved for the outer-sphere correlation.

In contrast, the inner-sphere, superoxide binding pathway, must utilize a folding motif generating a six-coordinate intermediate in which one of the NH's on the side with two cis NH's folds into the pseudo-axial site. For all the complexes **1**−**17** we observed that there indeed exists a unique lower energy folded conformer. This is consistent with the possibility that the inner-sphere pathway employs a folded structure that is unique and different from the outer-sphere pathway, and it is consistent with the inner-sphere path being accessed by an intermediate common to the outer-sphere path. For example, one such scenario is that the outer-sphere path could involve folding one of the three cis NH's fold into an axial site, and the inner-sphere path would then utilize a vacant site on the opposite side of the plane of the Mn(L) complex and hence fold one of the two nonadjacent cis NH's into the axial site. Chemically, this could arise if the aquo six-coordinate complex, with a vacant

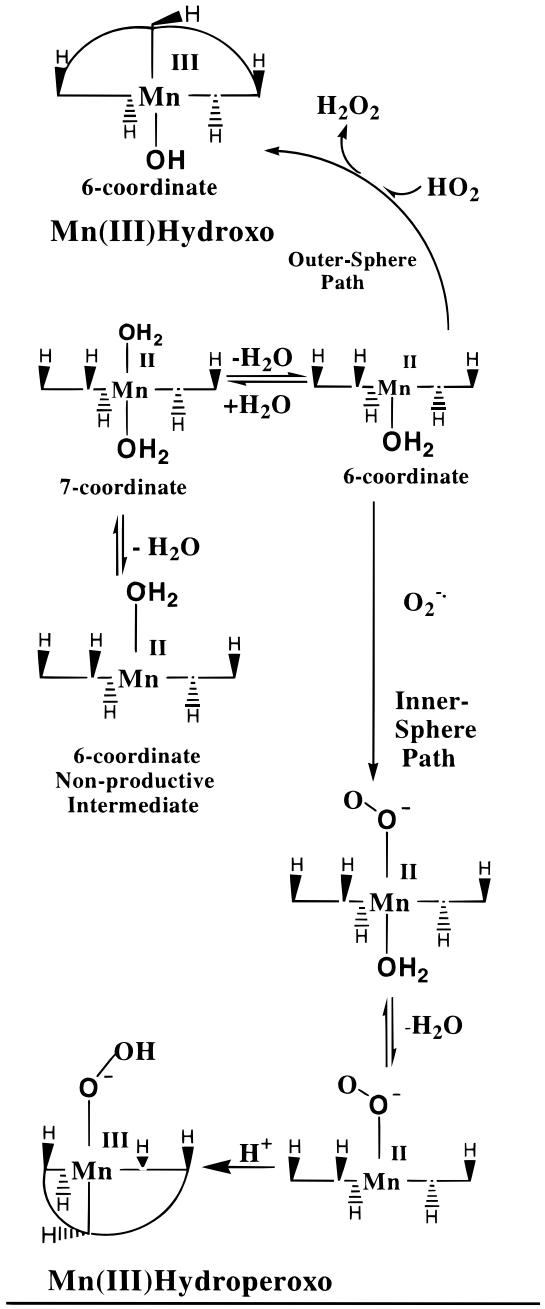

Figure 5. Mechanistic scheme depiction for the formation of a unique six-coordinate intermediate complex which gives rise to both the inner-sphere and outer-sphere pathways for oxidation of Mn(II).

coordination site on the side of the macrocyclic ring with three NH's cis, binds superoxide anion in this vacant site. Loss of the bound trans water and subsequent folding of either one NH's on the side of the two cis NH's would generate a folded six-coordinate pseudo-octahedral complex. This is the paradigm that evolved from the modeling efforts and will be described in more detail with the calculations described here.

At the outset we could make no claim as to the validity of this paradigm, other than it is consistent with the general mechanistic understanding and characterization of the chemistry of these complexes. The reaction scheme in Figure 5 depicts how such substitution processes as described here could account for the two types of folds leading to the two unique pathways for oxidation of Mn(II).

As noted above in the Introduction, the modeling exercise involves calculating the energy of the Mn(III) complexes for

Table 2

	$\Delta E^{\#}$ ($E_{Mn(III)} - E_{Mn(II)}$) (kcal)	
complex	inner-sphere	outer-sphere
1	9	14.7
2	7.6	11.1
3	7.9	12.4
4	3.2	22.2
5	26.3	18.0
6	8.3	19.0
7	2.2	25.0
8	3.5	6.3
9	20.0	20.1
10	2.5	38.9
11	11.9	7.8
12	8.0	9.8
13	8.8	22.3
14	8.3	12.4
15	4.9	18.8
16	3.4	16.9
17	15.8	10.6

all combinations of the three NH's folding for the outer-sphere path and for each of the two NH's folding for the inner-sphere path. Then the energies of the corresponding structures with Mn(II) are calculated. The lowest energy folded Mn(II) structure provides the basis for the lowest ΔE ($E_{Mn(III)} - E_{Mn(II)}$) fold for each of the two paths. In general, we find that there is a clear energy preference for a single, unique NH to fold on each side of the macrocycle for both pathways—the energy differences between possible NH folding modes were large (sometimes as large as 70−100 kcal); thus, ΔE ($E_{Mn(III)} - E_{Mn(II)}$) for the three outer-sphere folds and for the two inner-sphere folds for each complex always affords a clear lowest energy choice for each type of fold with each complex. This is actually somewhat surprising at first glance, but it is clear from these modeling analyses that the orientation of the NH's is clearly an important aspect of the strain energies required to fold the ligands. This feature induces large ΔE differences for the different folds, even in a more symmetrical structure such as that of the unsubstituted complex **1**.

Implicit in this exercise is the assumption that the orientation of the NH's relative to the substituents is known. For those complexes in which crystallographic data exist, the orientations are known. Using these data, certain structural relationships (e.g., a *trans*-cyclohexano substituent dictates that the NH's α to the substituted carbons of the macrocyclic ring must also be *trans*), and MM calculations of the free ligands and for the Mn(II) planar 7-coordinate complexes, the NH pattern can be established with a high level of confidence for all 17 of the complexes used in the database. Figure 2 shows all of these complexes with the orientation of the NH's and shows the NH's which fold (N^O, N which folds for outer-sphere path; N^I, N which folds for inner-sphere path). In Table 2 are listed the lowest energy difference values for each complex for each type of fold (inner-sphere and outer-sphere): ΔE ($E_{Mn(III)} - E_{Mn(II)}$). These data are depicted graphically in Figures 6 and 7 for the inner- and outer-sphere paths, respectively.[17] Clearly, the relative ease of folding of the macrocyclic ligand to generate a pseudo-octahedral geometry correlates with the rate data for the folding, which we have ascribed to the inner-sphere and to the outer-sphere fold. The catalysts that operate efficiently via an outer-sphere or inner-sphere mechanism show a very low energy difference between the Mn(III) and Mn(II) folded conformers for each respective fold. That there is such a good agreement

(17) The outlying points in Figures 6 and 7 correspond to complexes **5** and **7**, respectively.

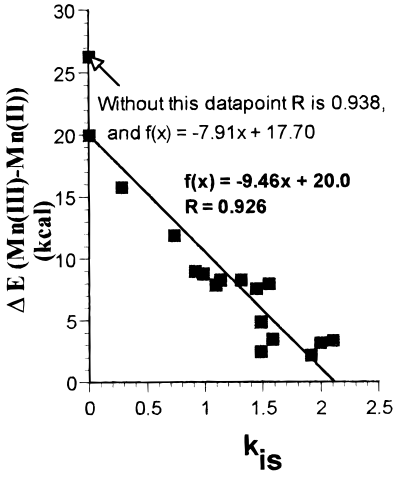

Figure 6. Correlation of the lowest $\Delta E^{\#}$ from MM calculations for the folding of an NH on the side of the two NH's into the axial site with the experimentally derived inner-sphere rate constants, k_{IS}.

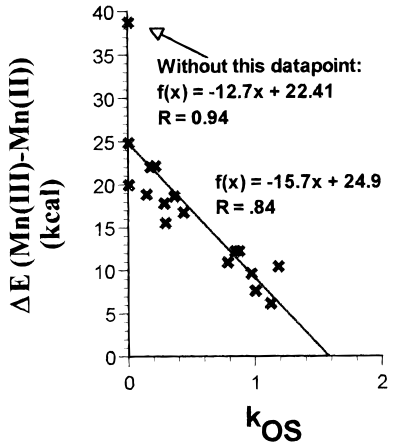

Figure 7. Correlation of the lowest $\Delta E^{\#}$ from MM calculations for the folding of an NH on the side of the three NH's into the axial site with the experimentally derived outer-sphere rate constants, k_{OS}.

provides support for the detailed mechanistic pathway proposed here. In fact, if there were random modes of folding such that any NH fold could be associated with either pathway, there would exist a random array of data. Additionally, if the structure of the productive intermediate in Figure 5 is the 6-coordinate complex, which possesses the vacant coordination site on the side with the two cis-nonadjacent NH's, then the correlation would totally break down—in fact, give the reverse to what is observed.

Given that this correlation exists, the real utility would be in the ability to design highly substituted, stable complexes that are highly active on the basis of the modeling data alone. Thus, the chemistry would not need to rely on trial and error synthesis, which can be exceedingly time-consuming for the synthesis of such highly substituted and stereodefined ligands, to find a stable complex with high catalytic activity. The molecules **18**−**21** were synthesized as a test of this modeling paradigm. In Table 3 the calculated energies for the two types of folds generated as described above are listed. From the standpoint of ease of synthesis and the desire to maximize the stability with the minimum number of substituents, we chose to further elaborate the bis(cyclohexano) structure of the high activity catalyst, complex **8**. Note that this complex (with four of the macrocyclic ring carbons bearing a substituent) achieves stability equivalent to those complexes (**14**−**17**) bearing five substituents. Thus,

Table 3

complex	$\Delta E_{IS}^{\#}$ ($E_{Mn(III)} - E_{Mn(II)}$) (kcal)	k_{IS} (calcd)[a]	k_{IS} (Exp)	$\Delta E_{OS}^{\#}$ ($E_{Mn(III)} - E_{Mn(II)}$) (kcal)	k_{OS} (calcd)[a]	k_{OS} (Exp)
18	11.3	0.81	0.98	15.8	0.52	0.53
19	11.1	0.83	0.57	5.0	1.37	1.80
20	22.2	0	0.15	29.7	0	0
21	13.6	0.51	0.39	12.6	0.77	0.45

[a] These k values were calculated using the modified correlation equations of fit for inner-sphere ($\Delta E^{\#} = -7.91k_{IS} + 17.7$) and outer-sphere ($\Delta E^{\#} = -12.74k_{OS} + 22.41$).

synthetically, it was attractive to add an additional methyl to this structure (**8**). Intuitively, to increase the stability most efficiently, we chose to put the additional substituent on one of the chelate rings that did not possess a substituent. Thus, structures **18** and **19**, each bearing an additional methyl substituent, were modeled. The two complexes only differ in the stereochemistry of the added methyl substituent: **18** (*S*-Me) and **19** (*R*-Me). The predictions based on the use of these correlations are that the all *R* complex **19** should be a very good catalyst, especially via the outer-sphere pH dependent path, while complex **18** with the *S*-Me would be much less active via this mode, and they should possess comparable activities via the inner-sphere path. As predicted, complex **19** is in fact very active with a large pH dependence; at least 3 times that of complex **18**. In fact, complex **19** possesses a catalytic rate at pH = 7.4 in excess of 1×10^8 M^{-1} s^{-1} and was the most active catalyst synthesized up to that point. The predictions were not quite so compelling regarding the inner-sphere path. Although the predicted rates were roughly comparable, the rate via the inner-sphere path (the minor contributor to the overall rate for these two catalysts) for complex **19** was actually observed to be less than that of **18**.

Based of this level of success, it was intriguing to consider more highly substituted structures and whether they, in fact, would have catalytic activity. One type of substituent that we have observed to enhance stability is the *gem*-dimethyl; thus the *gem*-dimethyl complex **20** (the analogue of **18** and **19**) was subjected to the modeling paradigm. The results were quite clear; namely, there did not exist any folds that are of a low energy. In other words, neither the inner- or outer-sphere pathway would be predicted to operate with this structure. The ligand and complex were synthesized, and indeed, only a trace of catalytic activity was observed.

The desire to increase stability by increasing the number of substituents on the macrocycle while retaining good catalytic activity led us to consider whether there were carbons of complex **19** (our most active catalyst) on which one could add a substituent and retain good activity. This exercise utilizing the modeling led to the prediction that, of the five carbon atoms of the macrocyclic ring of **19** that were devoid of substituents, the 14-position could bear a methyl (or other substituent) and retain reasonable activity, but only if the stereochemistry of that additional substituent is *R*—generating the all *R* hexasubstituted ligand structure **21**. The modeling, in fact, predicts that the catalytic activity for such a complex **21** should be midrange within this family via both pathways. The actual activity was not quite as high as predicted but was nevertheless very good considering that the complex bore six substituents. In fact, this complex has better activity than the original unsubstituted parent complex **1** and has a kinetic stabilty of over 2000 times that of **1**. Figures 8−10 show respectively the predicted planar 7-coordinate Mn(II) complex geometry, the folded outer-sphere 6-coordinate geometry, and the folded inner-sphere 6-coordinate geometry of this complex, **21**, as its Mn(II) chloro complex. An inspection of these figures reveals an important structural insight into the driving force for the folding. The 14*R*-Me substituent is in an axial position in the planar 7-coordinate structure. This higher energy conformation is dramatically relieved when the outer-sphere fold occurs, generating the

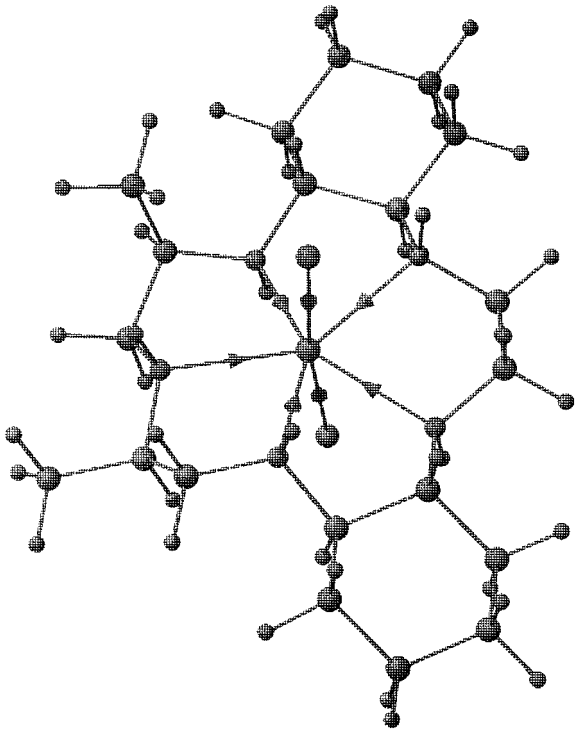

Figure 8. Predicted structure from MM calculations of the *trans*-dichloro Mn(II) complex, **21**.

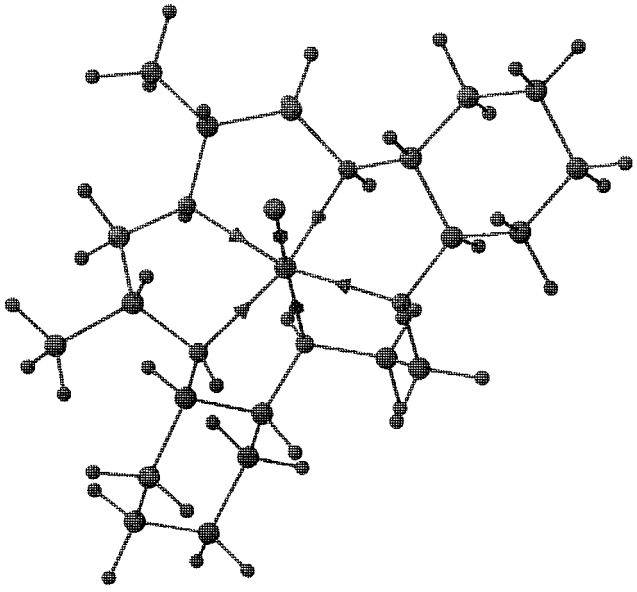

Figure 9. Predicted lowest energy structure from MM calculations of the folded six-coordinate chloro Mn(II) complex derived from structure **21** showing the outer-sphere fold.

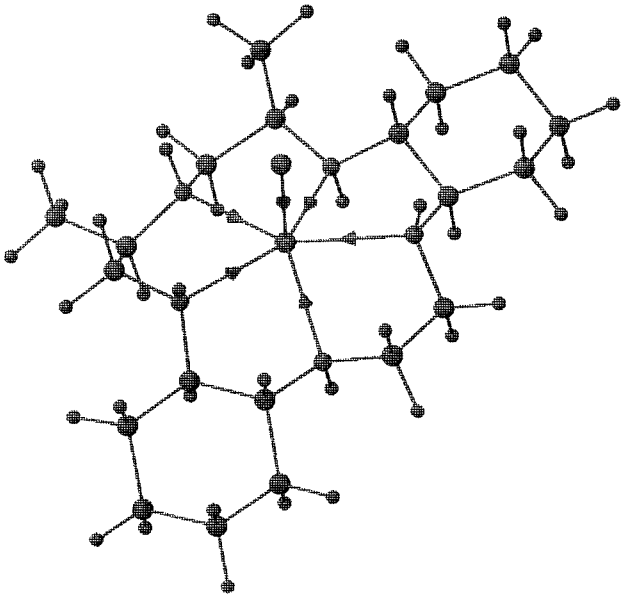

Figure 10. Predicted lowest energy structure from MM calculations of the folded six-coordinate chloro Mn(II) complex derived from structure **21** showing the inner-sphere fold.

6-coordinate structure of Figure 9. This folding places the 14*R*-Me in an equatorial orientation, thus relieving strain and providing a driving force for the fold.

The results of the modeling for this complex (**21**) are given in detail as an illustrative example of the process to which all of the complexes were subjected. The details of the energy calculations for the Mn(II) and Mn(III) folded structures for the inner- and outer-sphere paths and for the planar seven-coordinate Mn(II) structure (all as chloro complexes) are listed in Table 4 for **21**. They reveal that the major factor determining the total energy for a particular complex generated via the MM calculation is largely governed by angle strains, dihedral strain, and van der Waals interactions—not H-bonding effects, as they are nearly invariant across all the complexes. Additionally, within this entire family of complexes the electrostatic contributions to the *E* value of all Mn(II) complexes is nearly constant around 1−2 kcal and the contribution for all the Mn(III) complexes is similar at 27−28 kcal. Thus, the assumption that in a first approximation these two terms cancel out in the correlation is seen to be valid.

Table 4

contributions to E_{tot} (kcal)	7-coord Mn(II)	$Mn(III)^{OS}$	$Mn(II)^{OS}$	$Mn(III)^{IS}$	$Mn(II)^{IS}$
electrostatics	2.98	−27.2	1.92	-28.4	1.16
stretch	2.52	5.11	3.11	4.65	2.76
bend	0.77	1.5	1.09	1.16	0.94
improper torsion	0	0	0	0	0
angle strain	10.6	36.7	12.1	36.1	10.4
dihedral strain	11.0	27.6	18.6	22.4	13.0
Van der Waals	14.4	21.7	16.2	21.2	14.9
H bonding	−1.91	−1.53	−1.73	-1.54	−1.18
total	40.4	63.8	51.2	55.5	41.9

In general, the linear correlations developed for this system of Mn(II) complexes lend support to the theory that folding is a critical aspect of catalytic activity for these synthetic enzymes ("Synzymes") and that substituents (relative position and stereochemistry) influence the favorability of the folding in a predictable manner. Thus, we are able to model any given complex for both the inner-sphere or the outer-sphere folding energetics and calculate the expected rate constant for each path for any ligand pattern! This paradigm has worked extremely well at correlating and predicting activity and has made it possible to design highly complicated molecules and test their potential utility as a catalyst without the extraordinary effort required to first synthesize such a structure. We have been able to literally test hundreds of combinations of structures in this fashion and been able to gain a fair degree of certainty regarding a structure prior to embarking on the complicated synthesis. In no case have we yet observed this MM modeling paradigm to fail to predict the approximate activity of a complex. Indeed, we have modeled and synthesized many more structures and have been able to synthesize synzymes with increased stability (more than a factor of 100× from that of complex **21**) and with catalytic rates exceeding 10^9 M^{-1} s^{-1}.[16]

Acknowledgment. The authors would like to thank Mr. Hayat Rahman, Mr. Willie Rivers, and Mr. Kirby Sample for their outstanding technical assistance.

IC981319B